

Acoustic backscattering at low grazing angles from the ocean bottom. Part II. Statistical characteristics of bottom backscatter at a shallow water site

N. P. Chotiros, H. Boehme, T. G. Goldsberry, S. P. Pitt, R. A. Lamb, A. L. Garcia, and R. A. Altenburg

Applied Research Laboratories, The University of Texas at Austin, P. O. Box 8029, Austin, Texas 78713-8029

(Received 21 June 1984; accepted for publication 2 October 1984)

Analyses of the statistical characteristics of bottom backscatter, measured in shallow water off San Diego, California, are presented. (The initial results of the experiment were presented by T. G. Goldsberry, S. P. Pitt, and R. A. Lamb at the 104th Meeting of the Acoustical Society of America, Orlando, FL, 8–12 November 1983.) The experimental sonar, mounted on the sea bottom, was operated at 30 kHz to gather data over a wide sector of the bottom. The bottom was patches of coarse and fine sand. The distribution function and probability of false alarm function of the detected envelope of widebeam and narrowbeam signals were measured. Some spatial and temporal correlation functions of the signal amplitudes were measured. A limited attempt was made to compare the results with existing theoretical models.

PACS numbers: 43.30.Bp, 43.30.Gv, 92.10.Vz, 91.50.Ey

INTRODUCTION

Underwater acoustic bottom backscattering at audio and ultrasonic frequencies has been measured and reported by McKinney and Anderson,¹ Wong and Chesterman,² Urick,³ and Muir *et al.*⁴ The main objective of these measurements was to estimate the level of the backscattering strength. Estimates of the statistical characteristics, such as distribution functions and correlation functions, were limited. These functions received more attention in surface backscatter, however.^{5–7} Recently, the probability density of bottom backscatter in a freshwater lake has been reported by Wilson and Powell.⁸ The scattered pressure density function was estimated, and it was concluded that the density function differed significantly from a Gaussian function, particularly in its heavy tails.

In this paper, temporal and spatial correlation functions, distribution functions, and the probability of false alarm functions of the backscattering strength at a site on the West Coast were estimated for grazing angles less than 10°. Their dependence on beamwidth, azimuth, range, and motion was examined. At this stage no attempt has been made to fit a theoretical model to the results. The correlation function of the signal power at the output of an ideal square law detector, rather than the signal pressure, was computed. The distribution function of the detected signal power was computed rather than the pressure statistics. A sufficiently large number of data samples were taken to allow sensitive estimates of the distribution function to be made. The distribution functions were compared using the Kolmogorov–Smirnov (K–S) test to check for stationarity. Of particular interest was the probability of false alarm (PFA) functions, defined as one minus the distribution function. The measured PFA curves were compared with the Rayleigh model and a log-normal model with a standard deviation of 5.57 dB. The functions were plotted as a function of the log of the signal power in decibel units rather than in linear values. This has the advantage that a change in amplifier gain, results in a simple shift of the curve without distortion, and allows ran-

dom processes of different scales but of the same distribution to be identified. More generally, the results were presented in this form because it is more appropriate for signal processing applications.

The data used are a subset of bottom backscatter data recorded off Mission Beach, San Diego, California, in May 1982.⁹ Although data were recorded at a number of carrier frequencies, only the 30-kHz data were sufficiently abundant for detailed analysis. The results presented here were obtained with a 0.25-ms cw pulse at a carrier frequency of 30 kHz. The data sets used came from two recording sessions; one was a recording of bottom reverberation from a fixed position, and the other was a recording taken while the sonar was slowly and uniformly rotated about a vertical axis. The former will be referred to as the “fixed azimuth data” and the latter as the “scan” data. In each case, the maximum response axis (MRA) was directed downward at a depression angle of 5° and both wide (21°) and narrow (2.8°) receive beams were used simultaneously. The vertical beamwidth was 10° in both cases. The signal was a 0.25-ms cw pulse. Due to surface backscatter contamination, the scan data were valid out to a range of only 70 m. The fixed azimuth data, which were taken on a calmer day, were valid for ranges up to 100 m. A more detailed description of the site and experimental conditions is given in Part I of this two-part series.

The flexibility of the system was somewhat limited by the fact that the sonar was mounted on a fixed platform at a height of 4.5 m above the bottom. Consequently some operating parameters, such as range and grazing angle and bottom patch and azimuth angle, were not separable. However, the fixed platform contributed to the repeatability of operating parameters and the high degree of stability that increased the accuracy of the statistical analyses.

Two bottom types were represented by the data. The fixed azimuth data were taken over a fine sand bottom. The scan data spanned a large azimuth sector which included both fine sand and coarse sand. A summary of the bottom characteristics is shown in Table I.

TABLE I. Measured properties of the two types of sand bottom at the San Diego site.⁹

	Fine sand	Coarse sand	Units
Pressure velocity ratio	1.10	1.15	
Acoustic attenuation	0.47	0.29	dB/m-kHz
Specific density	1.9	2.2	
Mean grain size	8.8×10^{-5}	54×10^{-5}	m
rms height fluctuation	9×10^{-3}	22×10^{-3}	m

I. THE CORRELATION FUNCTION

The correlation functions were computed as functions of the signal power. The instantaneous signal amplitude $x(i)$ was estimated by taking the Hilbert transform of the recorded data samples, and then taking the modulus of the resulting complex time series. The instantaneous signal power is directly proportional to the square of the amplitude $x^2(i)$.

The normalized power crosscorrelation estimate $C_p(\tau)$ between two sets of time series power samples $x^2(i)$ and $y^2(i)$ was defined as follows:

$$C_p(\tau) = \left(\sum_{i=M}^{M+N} x^2(i) y^2(i + \tau) \right) / \left(\sum_{i=M}^{M+N} x^4(i) \sum_{i=M}^{M+N} y^4(i) \right)^{1/2}, \quad (1)$$

where N is the sampling window, M is the sample number of the first sample within the window, the time shift τ is equal to $r\Delta t$, r is an integer, and Δt is the data sampling period. This definition of the crosscorrelation function is particularly relevant to signal detection analysis since it is directly applicable to the output signal of an ideal square law detector.

In the special case where $x^2(i)$ and $y^2(i)$ are samples of stationary random processes (X^2 and Y^2), and if the first and second moments of the two random processes are equal, then the following relationship applies.¹⁰

$$E[C_p(\infty)] = m_1^2 / m_2, \quad (2)$$

where m_1^2 is the square of the first moment, and m_2 is the second moment. $E[\dots]$ denotes the expectation value. Furthermore, for Rayleigh random processes,¹⁰

$$E[C_p(\infty)] = m_1^2 / m_2 = 0.5. \quad (3)$$

Of course, if the two processes were also completely correlated, then

$$C_p(0) = 1. \quad (4)$$

In all of the following crosscorrelation results, the number of points N was 250.

A. The autocorrelation function

The autocorrelation function was measured over several sections of the reverberation data. Estimates of the autocorrelation functions were computed using Eq. (1) with $x = y$. Typical examples of the widebeam sample function $x(i)$ and its power autocorrelation function are shown in Fig. 1. Note that $C_p(\tau)$ for large values of τ varies about a mean value of 0.5, which suggests that it may be a Rayleigh process.

However, the narrowbeam data shown in Fig. 2, recorded simultaneously with the data in Fig. 1, produced a

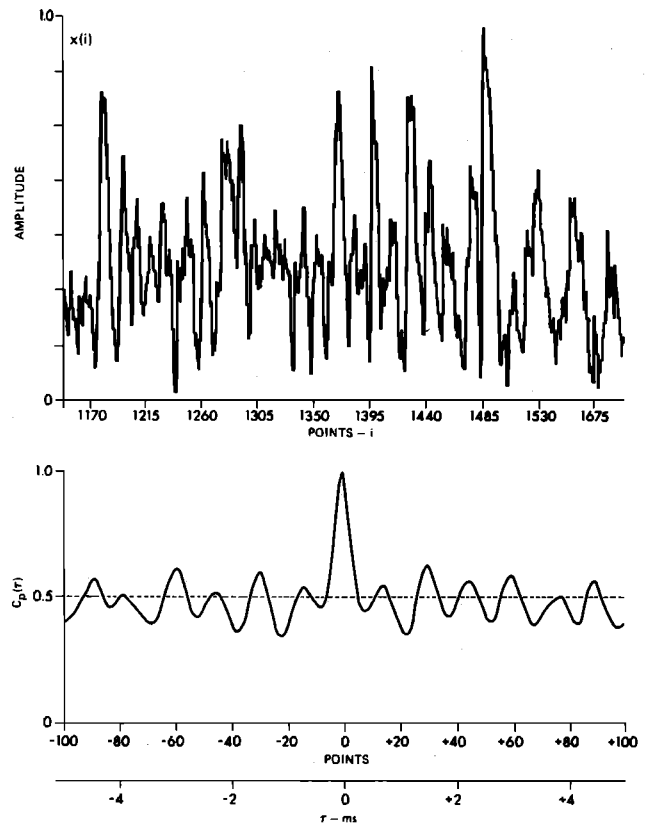


FIG. 1. A typical section of bottom reverberation time series samples $x(i)$ and its autocorrelation $C_p(\tau)$ from a 0.25-ms cw pulse, at 30 kHz and an azimuth beamwidth of 21° .

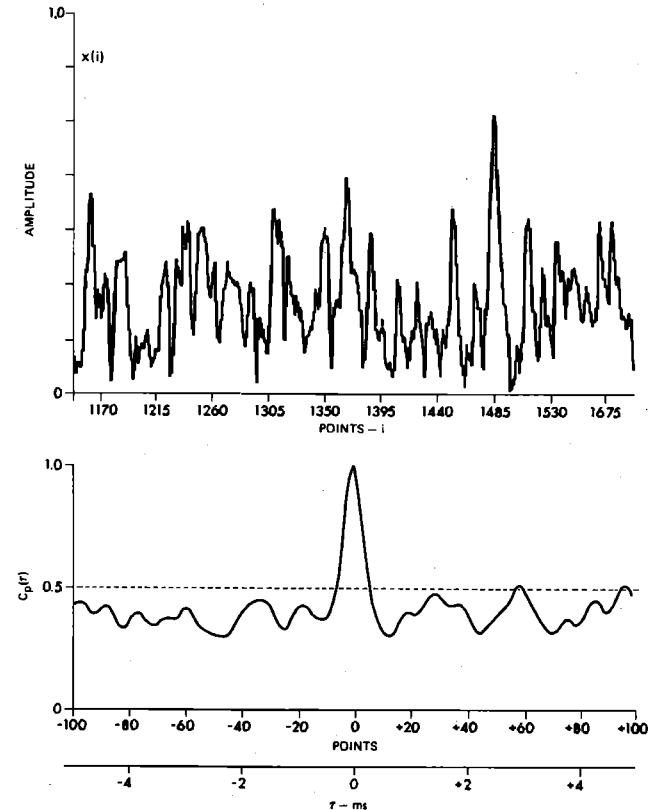


FIG. 2. A typical section of bottom reverberation time series samples $x(i)$ and its autocorrelation $C_p(\tau)$ from a 0.25-ms cw pulse, at 30 kHz and an azimuth beamwidth of 2.8° .

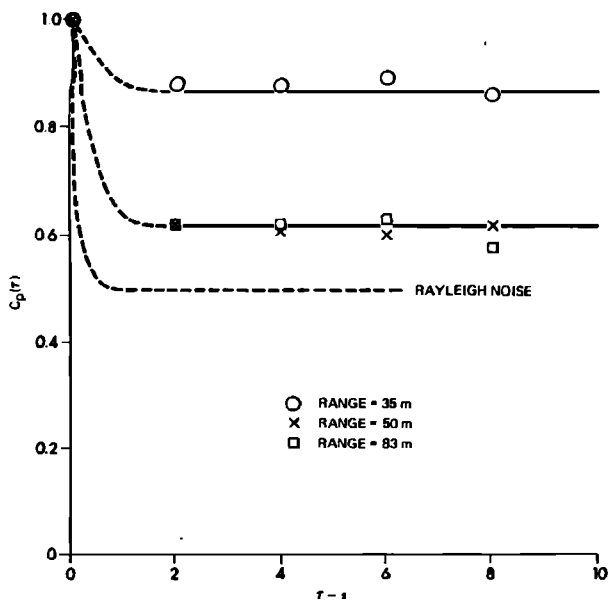


FIG. 3. Ping-to-ping crosscorrelation measurements at 30 kHz, with fixed azimuth data showing the effects of medium fluctuations at three ranges. Measurements were made with an azimuth beamwidth of 21°.

markedly different result. For the narrowbeam data, $C_p(\tau)$ for large values of τ varied about a mean value less than 0.5. This suggests that the narrowbeam process was non-Rayleigh. These results support the results of the probability of false alarm measurements, which also indicated that the process was significantly non-Rayleigh.

B. Temporal correlation function

The ping-to-ping power crosscorrelation was measured to determine the temporal stability of the reverberation. Figure 3 shows the power crosscorrelation functions of the widebeam data at a fixed azimuth, from three range intervals centered at 35, 50, and 83 m.

The results suggest that changes within the medium were occurring significantly faster than the ping repetition rate, thus producing a component of random variation between adjacent pings. This component as a proportion of the total variations appeared to increase with range. The results show that correlation between pings was small but not totally destroyed at the ranges of 50 and 83 m, since the values of $C_p(\tau)$ were still significantly higher than 0.5. It is interesting to note that random changes in the medium can significantly decorrelate the reverberation power between adjacent pings.

The corresponding results for the narrowbeam data, gathered simultaneously, are shown in Fig. 4. Both Figs. 3 and 4 show a similar degree of decorrelation and the same trend of increasing decorrelation with range, but the transition from higher to lower levels of correlation occurred at a longer range in Fig. 4. This seems to suggest that random changes in the medium do not affect widebeam and narrowbeam signals in exactly the same way. This is a reasonable assumption from the point of view of weak scattering theory. The perturbing influences within the medium may come in a very wide range of sizes: the acoustic signal is generally most sensitive to scatterers of a certain size, determined mainly by

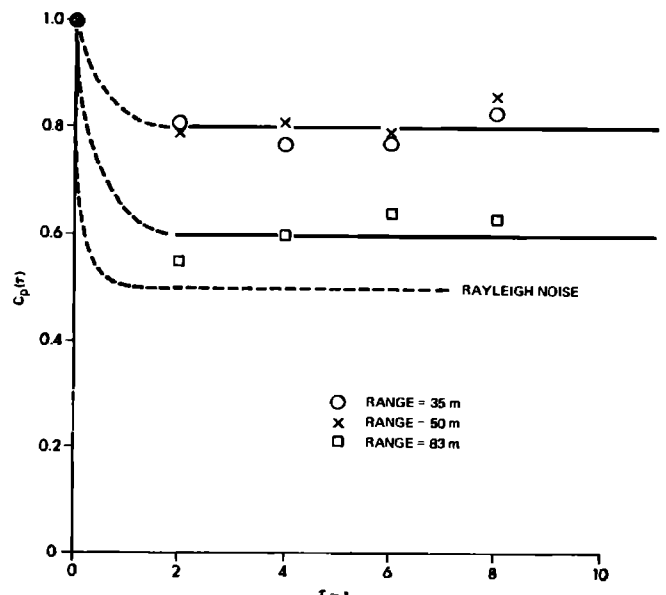


FIG. 4. Ping-to-ping crosscorrelation measurements at 30 kHz, with fixed azimuth data showing the effects of medium fluctuations at three ranges. Measurements were made with an azimuth beamwidth of 2.8°.

range and beamwidth.¹¹ Therefore, the widebeam and narrowbeam signals may be influenced by inhomogeneities in the medium of two distinct size ranges whose intensity and rate of change may be quite different.

C. Horizontal spatial correlation

An estimate of the horizontal correlation function of the backscattered signal field was obtained by measuring the crosscorrelation between signals from individual staves. However, it was found that, even between adjacent staves, no significant correlation was measurable. Consequently, it must be concluded that the horizontal correlation distances were much shorter than the staff center-to-center separation of 7.6 cm.

D. Azimuthal correlation

The ping-to-ping correlation was measured for the case where the sonar platform was slowly rotating about a vertical axis over a large azimuth sector. Assuming that the rotational axis passed through the acoustic center of the projector and receiver, the ping-to-ping correlation should simply be proportional to the degree of overlap of the insonified areas. After taking into account the decorrelation caused by medium effects, the results were found to support this hypothesis.

The results from the widebeam data, centered about two ranges, 35 and 50 m, are shown in Fig. 5. At a rotational speed of 0.8°/s and with an azimuth beamwidth of 21°, it would take 26 s to completely traverse one beamwidth and thus for the backscattered signals to originate from nonoverlapping areas. After accounting for the reduction in correlation due to medium effects from Fig. 3, the results show a steady decline in correlation in the interval 0–26 s at both ranges. The results from the narrowbeam data, measured simultaneously, are shown in Fig. 6.

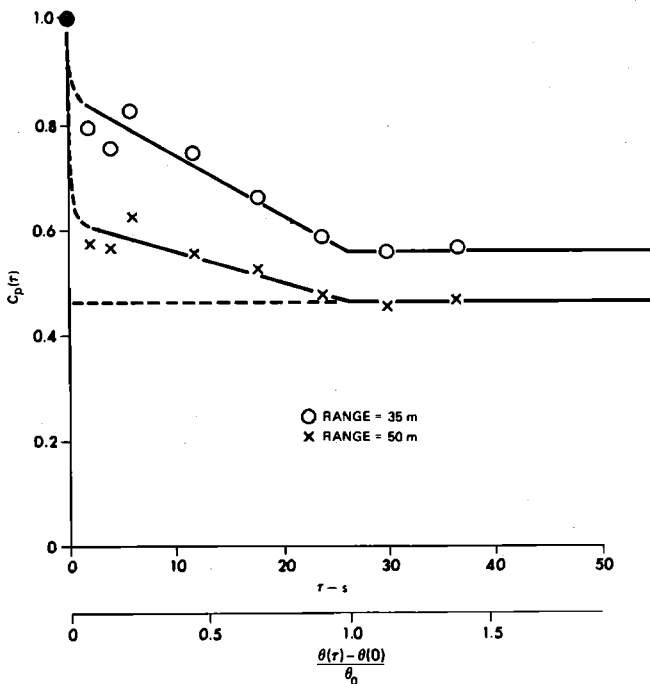


FIG. 5. Ping-to-ping crosscorrelation measurements at 30 kHz, with a slowly rotating platform. The azimuth beamwidth θ_0 was 21° . The angular velocity $d\theta/dt$ was $0.8^\circ/s$.

The asymptotic value of $C_p(\tau)$ was generally not equal to 0.5, being sometimes larger and at other times smaller. This is not surprising because the bottom reverberation strength was nonstationary; its mean value was found to vary with azimuth as described in Part I of this two-part series. The nonstationarity was also evident from the distribution function comparisons. Distribution function estimation and comparisons are described in the following sections.

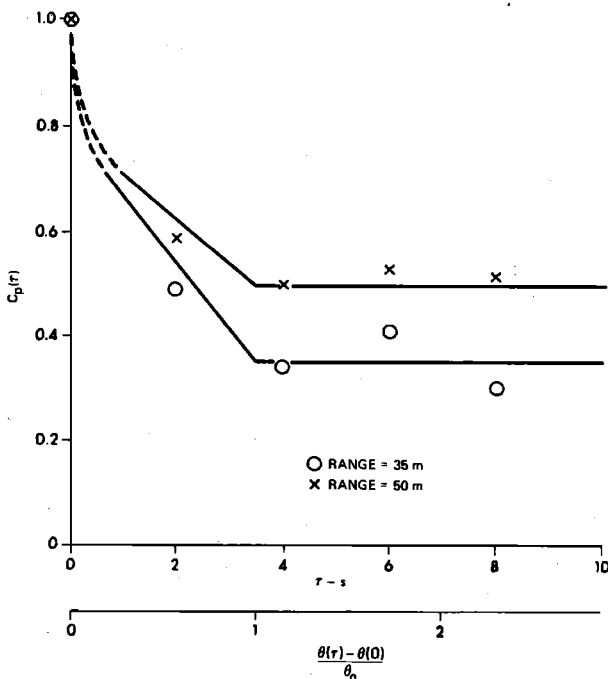


FIG. 6. Ping-to-ping crosscorrelation measurements at 30 kHz, with a slowly rotating platform. The azimuth beamwidth θ_0 was 2.8° . The angular velocity $d\theta/dt$ was $0.8^\circ/s$.

II. THE DISTRIBUTION FUNCTION

Each data sample was converted to the equivalent instantaneous bottom backscattering strength by adjusting for the transmit and receive sensitivities, the propagation losses, and the insonified patch area. The backscattering strength B_s was defined as the perceived target strength per square meter of the insonified area. The values of B_s obtained were found to follow Lambert's rule, i.e., they varied as the square of the sine of the grazing angle. Therefore a normalized backscattering strength B_0 could be obtained by removing the grazing angle dependence,

$$B_0 = B_s - 10 \log_{10}(\sin^2 \theta_g), \quad (5)$$

where θ_g = grazing angle.

The distribution function of B_0 , which is a logarithmic quantity, was computed. Using a logarithmic variable has the advantage that a change or error in a multiplicative process, such as in signal amplification, would only result in a shift of the distribution curve without any change in shape, and thus it is more tolerant of experimental inaccuracies of this nature. The logarithmic variable is also a logical choice of units to represent a random variable whose value may span several orders of magnitude.

A. Stationarity

By comparing the distribution function of B_0 , measured under different conditions, an attempt was made to assess the stationarity of the bottom backscatter as a random process.

The K-S two-tailed test^{12,13} was used to compare the measured distribution functions of B_0 by pairs. Any two distributions were deemed to be indistinguishable if they passed the K-S test at a confidence level of 5% or higher. The K-S test simply examines the maximum deviation between two distribution functions. If the maximum deviation exceeds the predetermined threshold for the number of independent samples and required confidence level, then the distributions are deemed to be different.

Using the scan data set, tests were carried out to determine if the statistics of B_0 were stationary with respect to changes in beamwidth, azimuth, range, and motion. The number of samples in each data set was approximately 3000. The results obtained are as follows.

B. Beamwidth dependence

The distribution function of a set of widebeam (21°) fixed azimuth data was compared to that of the corresponding set of narrowbeam (2.8°) data. Both sets of data were recorded simultaneously. The distribution functions passed the K-S test at the 5% level, indicating that they are indistinguishable. The curves are shown in Fig. 7. However, there are discernible differences, as will be shown later when examining the PFA curves.

C. Azimuth dependence

It was found that the distribution functions of B_0 from different azimuth angles consistently failed the K-S test. This indicated that the statistics of B_0 change as a function of

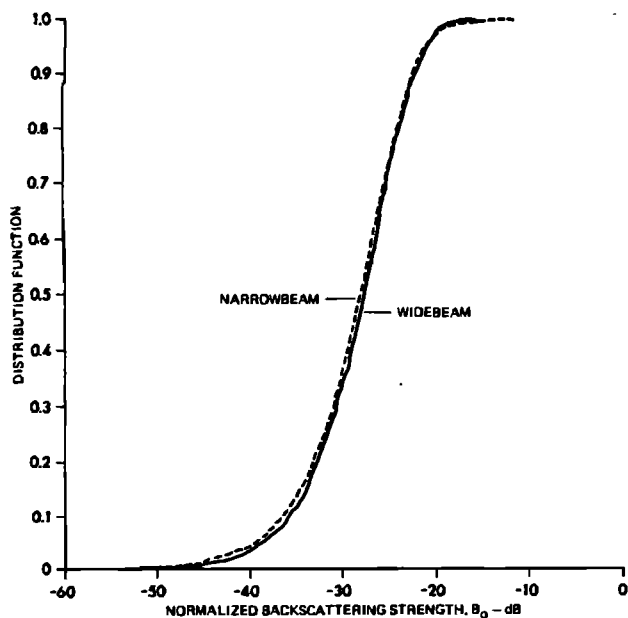


FIG. 7. Comparison of distribution functions from fixed azimuth widebeam (21°) and narrowbeam (2.8°) reverberation, over the range interval 80 to 101 m.

azimuth angle, and in this respect it was nonstationary. It has already been observed that the mean value of B_0 was dependent on azimuth angle; therefore this was not a surprising result.

Next, an attempt was made to determine whether the mean level of B_0 was the only statistic that was dependent on azimuth, or if the actual shape of the distribution function also changed. To compare the shapes of the distribution functions from different azimuth angles, it was decided that the mean level should be adjusted to 0 dB. The mean adjusted, normalized backscattering strength B_{00} was defined as

$$B_{00} = B_0 - 10 \log_{10}(\langle 10^{B_0/10} \rangle), \quad (6)$$

where $\langle \rangle$ denotes the ensemble average.

It was found that, over the homogeneous parts of the bottom, the distribution functions of B_{00} from different azimuth angles passed the K-S test at the 5% level. Therefore the difference in backscattering strength may be expressed in terms of a single gain factor which varied as a function of azimuth angle,

$$F_{B_0}(x) = F_{B_{00}}(x + a), \quad (7)$$

where x is the backscattering strength level in dB-m^{-2} and a is the offset in dB; the value of a is dependent on the azimuth angle.

From the scan data results, the value of a was found to vary smoothly from -33 to -26 dB, over a sector of 113° looking out over an area of coarse sand. This remarkable variation in level must have been caused by a highly directional scattering mechanism such as sand ripples.

D. Range dependence

Range dependence studies were hampered by surface backscattering contamination, which entered the mainlobe of the sonar directivity pattern via a bottom bounce path. At low grazing angles, the bottom was a highly reflective sur-

face. As a consequence, uncontaminated scan data of bottom backscattering were available for ranges less than about 70 m. The fixed azimuth data had been taken on a calmer day and were uncontaminated out to about 100 m. Within these limitations, the distribution functions of B_0 from different range intervals were compared. As with the azimuth dependence study, there were no detectable differences in the shape of the distribution functions. Small relative shifts in level of the order of 1 or 2 dB were required in some cases in order to pass the K-S test. This would indicate either a weak range dependence or small deviations from Lambert's rule. Since data were collected from a sonar on a fixed platform, at a constant height above the bottom, range and grazing angle dependences were not separable.

It is also possible that the change in mean level was only apparent, caused by inaccuracies in the measured sound-speed profile, which led to ray tracing errors and grazing angle estimation errors, and hence errors in the normalization process. Another possible cause would be changes in the bottom slope as a function of range. The bottom may not have been as perfectly planar as it was assumed to be. At a range of 80 m, the corresponding grazing angle was approximately 4° . At this value of grazing angle, a change in the bottom inclination of only 0.7° would produce a 1.3-dB error in the $10 \log(\sin^2 \theta_g)$ normalizing factor.

E. Motion dependence

It had been noted that the mean level of backscatter was azimuth dependent, and also weakly range dependent. Therefore the statistics of the data taken over a wide range of azimuth angles would be expected to be different from that taken from a fixed azimuth, and indeed they are. The distribution functions of narrowbeam (2.8°) data from the fixed azimuth data set and the scan data set were compared and they failed the K-S test at the 5% level. No amount of level adjustment could make them pass the test. Therefore the differences were not just due to level differences, but due to differences in the shapes of the curves. The results are shown in Fig. 8. However, since the two data sets were collected on different days, it was also possible that the differences may be due to changes as a function of time. Unfortunately, insufficient data exist to resolve this ambiguity.

III. THE PROBABILITY OF FALSE ALARM

For sonar performance analysis, the overall shape of the distribution function was relatively unimportant. The probability of small values of the PFA of 10^{-1} – 10^{-4} or even smaller are of direct interest. Therefore a logarithmic scale of PFA will be used. Up to this point, only distribution functions have been shown, and they all appear to be very similar to each other and to the Rayleigh distribution function. For the purposes of this study, the PFA is defined as one minus the distribution function,

$$\text{PFA}_{B_0}(x) = 1 - F_{B_0}(x).$$

On a logarithmic scale, the PFA function magnifies any anomalies which may exist in the upper-right-hand extremity of the distribution function. The PFA of the measured bottom backscatter data were analyzed as follows.

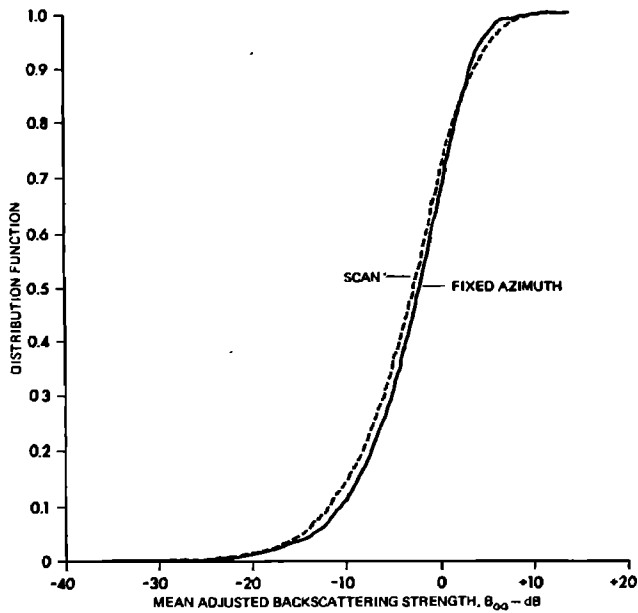


FIG. 8. Comparison of distribution functions from scan and fixed azimuth reverberation. The data were taken with a beamwidth of 2.8° .

The PFA of several data sets were compared by pairs. The predicted PFA of a Rayleigh model and that of a log-normal model¹⁴ with a standard deviation of 5.57 dB will also be shown below for comparison. The immediate objectives were to identify dependence on beamwidth, range, and azimuth.

A. Beamwidth dependence

The same pair of data sets used in the distribution function comparison were used in the PFA comparison. Although the distribution functions passed the K-S test and were therefore deemed to be indistinguishable, the PFA curves appear to be significantly different below a PFA of 10^{-2} . The results are shown in Fig. 9. They show an interest-

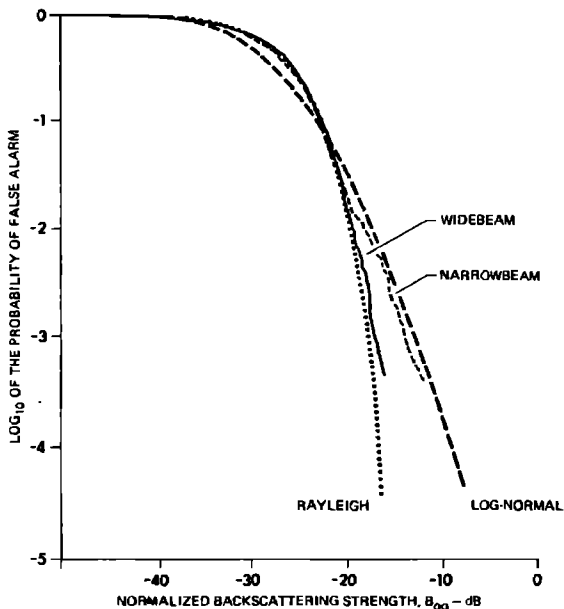


FIG. 9. Comparison of PFA from fixed azimuth widebeam (21°) and narrowbeam (2.8°) data at 30 kHz, over the range interval 80 to 101 m.

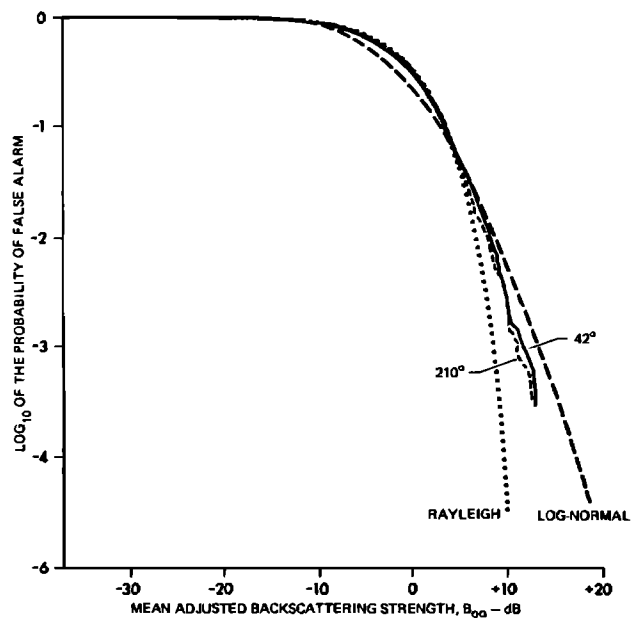


FIG. 10. Comparison of the probability of false alarms of reverberation from two sectors, centered about 42° and 210° bearing, respectively. In both cases, a narrowbeam (2.8°) was scanned over a sector 54° wide, and the range interval was 27 to 42 m.

ing deviation at low values of PFA which thus far has not been properly accounted for. Since the two sets of data were taken simultaneously over the same range intervals, the deviation must be entirely due to beamwidth differences or differences in the insonified areas. Interestingly, the widebeam data appeared to fit the Rayleigh model but the narrowbeam data tended to be log-normal. Similar results have been reported in radar backscattering studies.¹⁵

B. Azimuthal dependence

After adjusting for mean level differences, as had been done in the distribution function study, the PFA curves from different azimuths appeared to be very similar. An example is shown in Fig. 10. The data are a subset of the narrowbeam (2.8°) scan data. They have log-normal tendencies, which is consistent with the PFA curve of the fixed azimuth narrowbeam data in Fig. 9.

C. Range dependence

After adjusting for small differences in mean level, the PFA curves from different ranges, within the limits of the available data, appeared to be indistinguishable. As an example, the PFA curves of a pair of data sets are shown in Fig. 11. The data used are subsets of the widebeam (21°) fixed azimuth data, and they consistently appear to be more Rayleigh than log-normal.

D. Motion dependence

It has already been seen that the distribution functions from the fixed azimuth and scan data sets failed the K-S test and were considered different. It is therefore expected that their PFA curves would also be different. In the widebeam case, the PFA curves were significantly different. However, in the case of the narrowbeam data, the differences in the

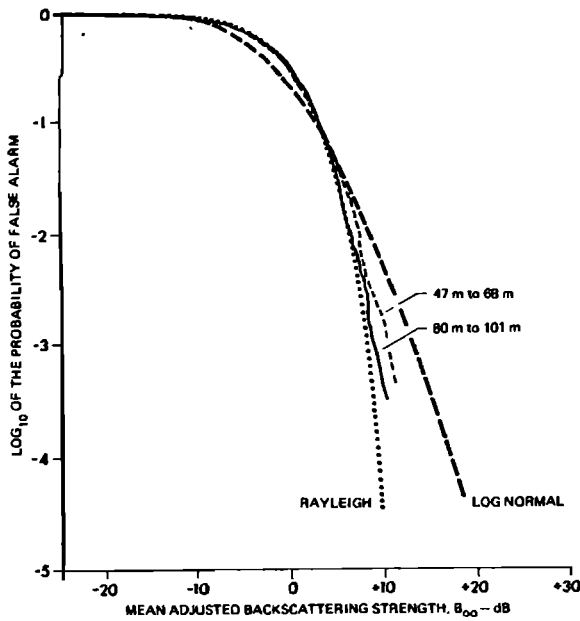


FIG. 11. Comparison of PFA of fixed azimuth data from two range intervals, 47 to 68 m and 80 to 101 m, respectively. The data were taken from a fixed platform, with a beamwidth of 21° , at 30 kHz.

PFA curves appeared to be small in that both have log-normal tendencies, as shown in Fig. 12, in spite of the differences in their distribution functions, as shown in Fig. 8.

Finally, the PFA curves of widebeam and narrowbeam scan data were compared to see the beamwidth dependence of data gathered from a wide azimuth sector. Both curves had log-normal tendencies, as shown in Fig. 13, unlike fixed azimuth data which showed a clear distinction between widebeam and narrowbeam. This result suggests that motion, in this case the scanning of the sonar over a wide sector, introduces nonstationarity to such a degree that it overwhelms the beamwidth dependence of the PFA function.

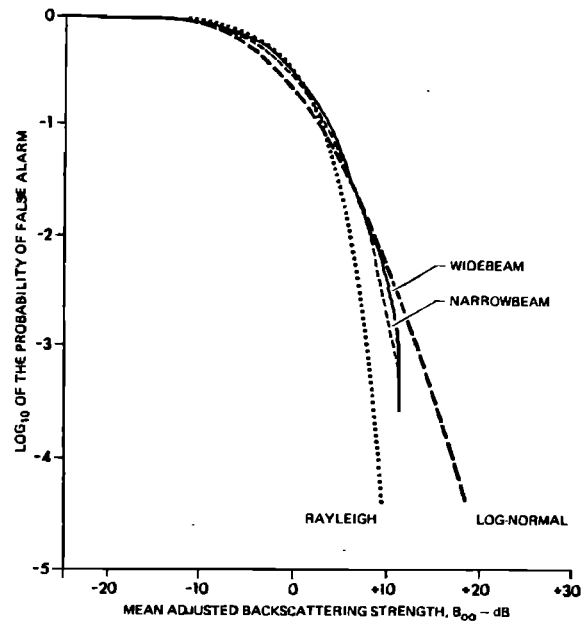


FIG. 13. Comparison of widebeam (16.5°) and narrowbeam (2.8°) data at 30 kHz, scanned over an azimuth sector approximately 150° wide, over a range interval of 27 to 48 m.

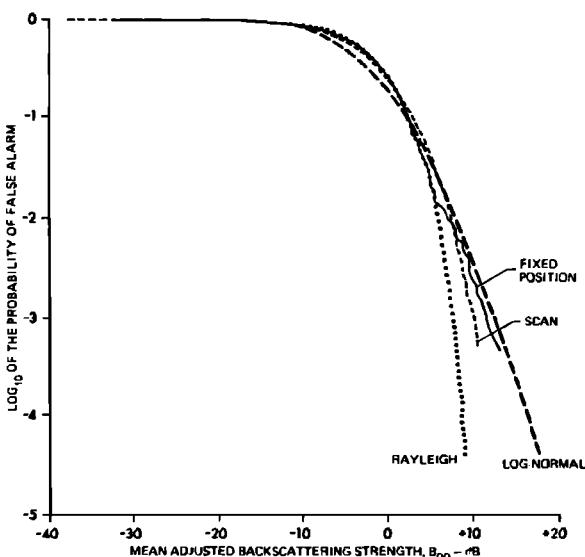


FIG. 12. Comparison of probabilities of false alarm from scan and fixed azimuth reverberation. The data were taken with a beamwidth of 2.8° .

IV. CONCLUSIONS

From autocorrelation function and probability distribution function measurements, it was found that the reverberation of a widebeam sonar (21°) from a uniform bottom area and at a fixed azimuth was consistent with the Rayleigh model. The agreement was good even at values of PFA as low as 10^{-3} . Reverberation measured simultaneously, but with a narrowbeam receiver (2.8°), showed a significant deviation from the Rayleigh model, particularly at low values of PFA, but the K-S test at the 5% level did not detect this difference.

Fluctuations from ping to ping were attributed to medium fluctuations. The component of medium induced fluctuations increased with range. The rate of increase with range was dependent on the sonar beamwidth, as well as on the medium characteristics. For this particular data set, fluctuations become the dominant component of the reverberation beyond a range of about 50 m. This suggests that ping-to-ping averaging may be used to remove a significant proportion of bottom reverberation even when the sonar position and attitude relative to the bottom is fixed.

From one bottom area to another, the distribution functions of the normalized backscattering strength remained constant in shape, but the mean level of the backscattering strength may shift depending on azimuth and position, as well as bottom type. The backscatter may be considered as originating from a common random process whose output is multiplied by a scaling factor which is position and azimuth dependent.

The distribution function of the normalized backscattering strength collected over a wide range of azimuth angles was characterized by nonstationarity. The distribution function of the ensemble, as well as the PFA function, appeared to be independent of beamwidth and definitely non-Rayleigh. They showed a log-normal tendency.

ACKNOWLEDGMENTS

This work was supported by NAVSEA Code 63R and NORDA Code 110A. The authors also wish to acknowledge the support of NOSC for the use of the oceanographic tower during the acoustic measurements. We also wish to acknowledge the consultation provided by Dr. John M. Huckabay, Dr. C. Robert Culbertson, and Garland R. Barnard during all phases of this work, and the efforts of Tracy Thompson in preparing the manuscript.

¹C. M. McKinney and C. D. Anderson, "Measurement of Backscattering of Sound from the Ocean Bottom," *J. Acoust. Soc. Am.* **36**, 158-163 (1964).

²H. K. Wong and W. D. Chesterman, "Bottom Backscattering Near Grazing Incidence in Shallow Water," *J. Acoust. Soc. Am.* **44**, 1713-1718 (1968).

³R. J. Urlick, "The Process of Sound Scattering at the Ocean Surface and Bottom," *J. Mar. Sci.* **15**, 134-148 (1956).

⁴T. G. Muir, Jr., R. S. Adair, J. G. Pruitt, and J. G. Willette, "A Geoacoustic Survey of the Brazos River, Part III: Reverberation Studies," Defense Research Laboratory Acoustical Rep. No. 294 (DRL-A-294), Defense Research Laboratory, The University of Texas at Austin (now ARL:UT), 17 April 1968.

⁵D. R. Jackson and K. Y. Moravan, "Horizontal Spatial Coherence of Ocean Reverberation," *J. Acoust. Soc. Am.* **75**, 428-436 (1984).

⁶G. R. Wilson and M. Frazer, "Horizontal Covariance of Surface Reverberation: Comparison of a Point-Scatterer Model to Experiment," *J. Acoust. Soc. Am.* **73**, 749-760 (1983).

⁷G. R. Wilson, "A Statistical Analysis of Surface Reverberation," *J. Acoust. Soc. Am.* **73**, 249-255 (1983).

⁸G. R. Wilson and D. R. Powell, "Probability Density Estimates of Surface and Bottom Reverberation," *J. Acoust. Soc. Am.* **73**, 195-200 (1983).

⁹M. D. Richardson, D. K. Young, and R. I. Ray, "Environmental Support for High Frequency Acoustic Measurements at the NOSC Oceanographic Tower, 26 April-7 May 1982; Part I: Sediment Geoacoustic Properties," NORDA Tech. Note 219, Naval Ocean Research and Development Activity, NSTL Station, Mississippi (June 1983).

¹⁰P. Z. Peebles, *Probability, Random Variables and Random Signal Principles* (McGraw-Hill, New York, 1980).

¹¹V. I. Tatarskii, *Wave Propagation in a Turbulent Medium*, translated by R. A. Silverman (McGraw-Hill, New York, 1961).

¹²F. J. Massey, Jr., "The Kolmogorov Test for Goodness of Fit," *J. Am. Stat. Assoc.* **48**, 1679-1684 (1951).

¹³S. Siegel, *Nonparametric Statistics for the Behavioral Sciences* (McGraw-Hill, New York, 1966).

¹⁴G. V. Frisk, "Intensity Statistics for Long Range Acoustic Propagation in the Ocean," *J. Acoust. Soc. Am.* **64**, 257-259 (1978).

¹⁵M. I. Skolnik, *Radar Handbook* (McGraw-Hill, New York, 1970), Chap. 26.